

Gluon-Induced Weak Boson Fusion

Robert V. Harlander⁽¹⁾, Jens Vollinga⁽²⁾ and Marcus M. Weber⁽³⁾

(1) *Fachbereich C, Bergische Universität Wuppertal, D-42097 Wuppertal, Germany*
 robert.harlander@uni-wuppertal.de

(2) *Theoretical Physics, NIKHEF, 1098 SJ Amsterdam, The Netherlands*
 jensv@nikhef.nl

(3) *Department of Physics, University at Buffalo, Buffalo, NY 14260-1500, USA*
 mmweber@buffalo.edu

The gluon-gluon induced terms for Higgs production through weak boson fusion (WBF) are computed. Formally, these are of NNLO in the strong coupling constant. This is the lowest order at which non-zero color exchange occurs between the scattering quarks, leading to a color field and thus additional hadronic activity between the outgoing jets. Using a minimal set of cuts, the numerical impact of these terms is at the percent level with respect to the NLO rate for weak boson fusion. Applying the so-called WBF cuts leads to an even stronger suppression, so that we do not expect a significant deterioration of the WBF signal by these color exchange effects.

PACS numbers: 14.80.Bn, 13.85.-t, 12.38.Bx

I. INTRODUCTION

One of the primary goals of the CERN Large Hadron Collider (LHC) is to find the mechanism for electro-weak symmetry breaking. The “standard” solution suggested many years ago predicts a fundamental scalar particle, called the Higgs boson (for reviews, see Refs. [1, 2, 3]). The interplay of extremely precise measurements and similarly precise calculations allows one to restrict its mass to the range between 114 and about 200 GeV [4] which is quite remarkable considering the fact that, a priori, this quantity is a free parameter of the theory. Unfortunately, the mass region below around 140 GeV turns out to be rather problematic for Higgs discovery at a hadron collider. The reason is that Higgs decay into weak gauge bosons is kinematically strongly suppressed, and the Higgs branching ratio into $b\bar{b}$ becomes dominant, reaching 70% at $M_H = 120$ GeV and more than 80% below $M_H = 100$ GeV. Without any additional tags from the production process, the signal is then completely swamped by the QCD production of $b\bar{b}$ pairs. Gluon fusion, which is the Higgs production process with the largest cross section at the LHC, does not provide such additional tags which is why one has to use it in combination with the rare decay into photons.

A few years ago it was pointed out that weak boson fusion (WBF) is very well suited for Higgs discoveries in the low mass region, provided that the kinematical distribution of the outgoing jets is properly identified [5]. The distinguishing feature of this process is the t -channel exchange of only color-less objects (weak gauge bosons), from which the Higgs boson is radiated. The signal therefore consists of two hard jets which can be found in opposite hemispheres of the detector at large rapidities, while the Higgs decay products are found at more central rapidities, without much more additional hadronic activity.

Even at next-to-leading order (NLO), color exchange among the scattering partons is strongly suppressed due to the fact that it requires a t - u -channel interference [6, 7, 8, 9, 10,

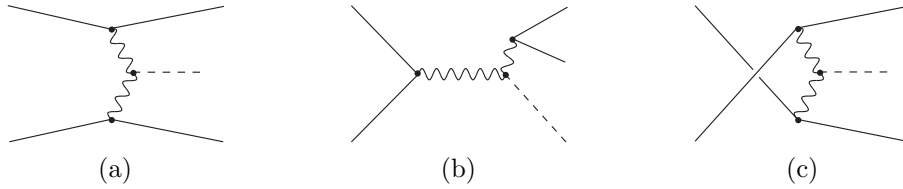


FIG. 1: Leading order contributions to (a) weak boson fusion and (b) Higgs-Strahlung; (c) is the crossed LO amplitude for WBF. The straight solid lines denote quarks (u, d, c, s, b), the wiggly lines denote W or Z bosons, and the dashed line means a Higgs boson.

11]. Thus, the next-to-next-to-leading order (NNLO) is the lowest order at which true color-exchange diagrams can contribute significantly to the WBF signal. The interesting issue is whether the jets produced by such a mechanism have similar kinematical distributions as the typical WBF jets. In this case, the color exchange might lead to additional soft radiation which could deteriorate the WBF signal.

Note that there is a process with the same final state $H + 2\text{jets}$ that does not involve weak gauge bosons: it is due to sub-processes like $gg \rightarrow Hgg$, for example, where the gluons couple to the Higgs boson via a top quark loop. Such terms are part of the NNLO contribution to gluon fusion [12, 13, 14] and must be considered as background when aiming for WBF. They were calculated at leading order (LO) in Ref. [15], where the full top-mass dependence was taken into account. The NLO terms were evaluated in the heavy-top limit [16].

The interference of this gluon fusion contribution to $H + 2\text{jets}$ with the WBF signal at NLO also leads to a net color exchange among the scattering partons and could diminish the virtues of the actual WBF signal. However, due to peculiar cancellations, the overall effect of these terms is negligibly small [17, 18].

The subject of this paper is the investigation and classification of color-exchange terms arising as radiative corrections to the fusion of weak gauge bosons. We identify a gauge-invariant, finite set of diagrams that shall allow us to provide an estimate of the size of such terms and thus their influence on the extraction of the WBF signal from experimental data.

The remainder of the paper is structured as follows: in Sect. II, we list the various NNLO contributions to the WBF process, identifying the class of diagrams that is relevant for our discussion, Sect. III describes technical aspects of the calculation, and Sect. IV contains our results. The conclusions are presented in Sect. V.

II. CLASSIFICATION OF THE DIAGRAMS

Typically, WBF denotes the electro-weak contribution to the process $pp \rightarrow Hjj$ that does not involve resonant weak gauge bosons. A tree-level example is shown in Fig. 1 (a). The contribution involving resonant weak gauge bosons, Fig. 1 (b), is usually referred to as Higgs-Strahlung. At tree-level, this distinction is theoretically well-defined. Experimentally, the two contributions can be distinguished by appropriate cuts: for example, in the

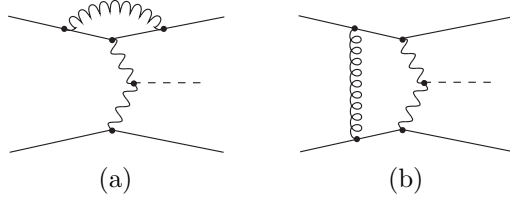


FIG. 2: NLO contributions to WBF: (a) DIS-like and (b) color-exchange diagrams. Notation for the straight and wobble lines is like in Fig. 1; spiral lines denote gluons.

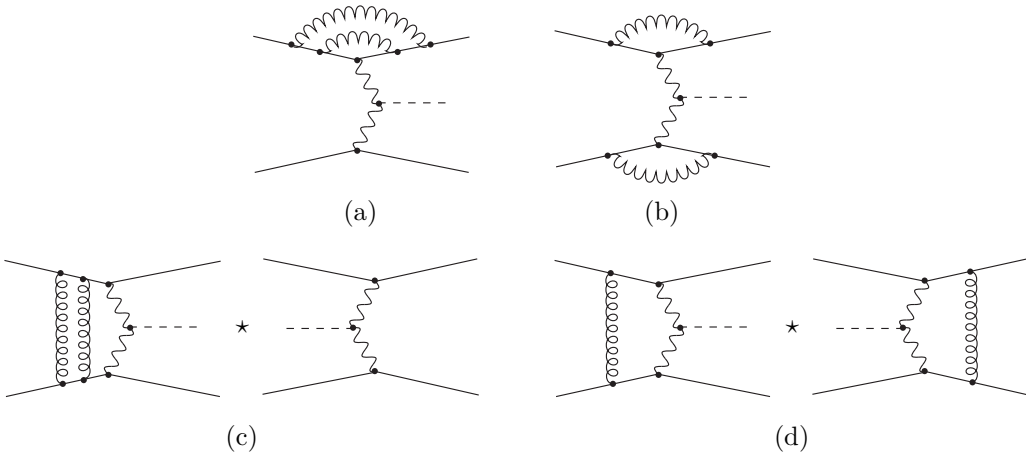


FIG. 3: NNLO QCD contributions to WBF: (a), (b) DIS-like diagrams and (c), (d) color-exchange contributions. Notation is like in Fig. 2.

WBF process, the two outgoing jets are typically produced with a much larger separation in rapidity than in Higgs-Strahlung where they arise from the decay of a massive gauge boson. At one-loop, on the other hand, the distinction between WBF and Higgs-Strahlung is less obvious, in particular for the purely electro-weak corrections. Therefore, in order to obtain the effects on the WBF process, Ref. [9] calculated the $\mathcal{O}(\alpha)$ and $\mathcal{O}(\alpha_s)$ corrections to the process $pp \rightarrow Hjj$ using the full set of diagrams and applied the cuts defined for the isolation of the WBF contribution.

When focussing only on the QCD corrections, a distinction between WBF and Higgs-Strahlung at NLO is still possible, since these terms are obtained by dressing the leading order diagrams with virtual or real gluons. The by far dominant QCD corrections to the WBF contribution come from DIS-like terms [6, 7, 8, 9], where the gluon modifies the $q\bar{q}V$ vertex, see Fig. 2 (a). Diagrams where the gluon connects the two quark lines, Fig. 2 (b), give no contribution when interfered with the uncrossed LO amplitude because of a vanishing color factor. On the other hand, the interference with the *crossed* leading order amplitude, Fig. 1 (c), is extremely small due to the strong forward-tendency of the outgoing jets [9].

This paper addresses the NNLO QCD corrections to the WBF process, i.e., terms of order $\alpha^3\alpha_s^2$ to $pp \rightarrow Hjj$ which do *not* involve resonant weak gauge bosons. Among them, we may still distinguish various contributions:

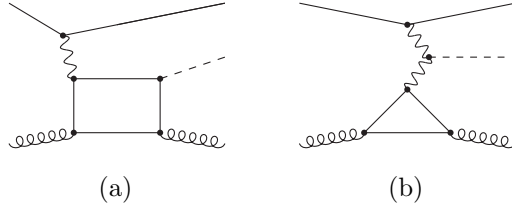


FIG. 4: Diagrams at $\mathcal{O}(\alpha^3\alpha_s^2)$ which involve closed quark loops. The notation is as in Fig. 2, except that the wiggly lines can only be Z bosons here, and the particle in the loop can be a top quark.

- DIS-like terms, i.e. those that merely involve corrections to the $q\bar{q}V$ vertex, see Fig. 3 (a),(b). Due to this similarity and because of the structure of the NLO results, we expect them to be similar in size as the NNLO corrections to the DIS process themselves [19].
- Diagrams involving gluon exchange between the two quark lines. Due to the possibility of two gluons forming a color-singlet state, the interference with the *uncrossed* amplitude is non-zero, see Fig. 3 (c),(d). Technically, the double gluon exchange diagram (c) is probably the most difficult one when aiming for the full NNLO result. Note, however, that the net color exchange is still equal to zero in this case. Thus, we do not expect this contribution to significantly increase the hadronic activity at central rapidities. It goes without saying that in order to arrive at infra-red finite results, all the above contributions require the calculation of single and double real gluon radiation.
- Diagrams involving closed quark loops, Fig. 4. Due to the smallness of the Yukawa couplings, only the top quark occurs in the loop of diagram (a). In diagram (b), on the other hand, only the third generation quarks survive the Furry theorem. Neither (a) nor (b) involves color exchange among the scattering partons. Note that crossing the external partons may lead to diagrams with a resonant weak boson and thus are not counted as WBF. In particular, the diagrams where both initial state particles are gluons were calculated in Ref. [20].
- Diagrams that involve only a single quark line, to be referred to as SQL diagrams in what follows. A generic set is shown in Fig. 5. The other terms of this class are obtained by simply crossing the external quarks and gluons, thus leading also to qg , $\bar{q}g$, and $\bar{q}q$ initial states.

Thus, the only diagrams involving a net color exchange among the scattering partons are Fig. 3 (d) and obvious variants, plus the SQL contribution. In order to get a handle on the size of the color exchange, in this paper we shall focus on the latter, i.e., the diagrams of Fig. 5. They form a gauge-invariant and UV-finite set and are IR finite without taking any real radiation into account. What also motivates the calculation of these diagrams is that they are the only ones through NNLO that involve purely gluonic initial states. Recalling that the gluon luminosity at the LHC is very large, one may expect their numerical impact to be rather sizable.

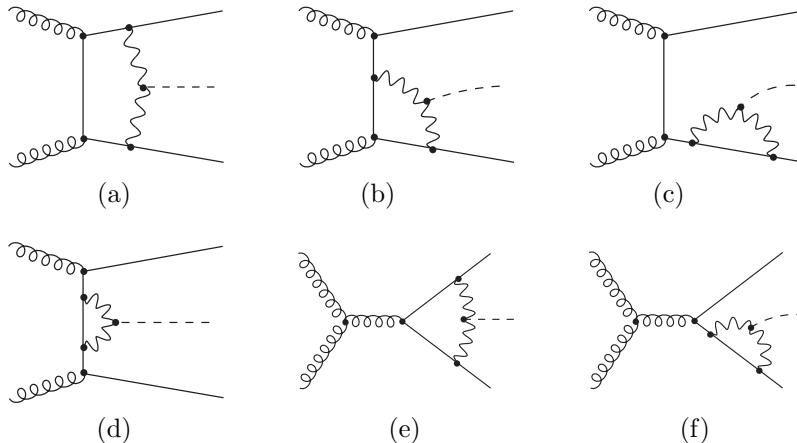


FIG. 5: NNLO contributions to WBF that contain only a single quark line. Shown are only the diagrams with purely gluonic initial state. qg , $\bar{q}g$, and $q\bar{q}$ initial state contributions are obtained from them by crossing the external quark and gluon legs. Notation is like in Fig. 2.

III. CALCULATION

The Feynman diagrams were generated using `FeynArts` [21, 22], taking into account the five light quark flavors, both in the initial and in the final state. In principle, the quark line in Fig. 5 could also be the top quark (for the gg channel), but we expect this contribution to be very small due to the large x values required for the incoming gluons and the reduced available phase space.

The Feynman diagrams are evaluated using standard techniques. The amplitudes are simplified with `FormCalc` [23] and the results in terms of Weyl-spinor chains and coefficients containing the tensor one-loop integrals have been translated to `C++` code for the numerical evaluation. The one-loop integrals are reduced to a set of standard integrals numerically. The 5-point integrals are written in terms of 4-point functions following Ref. [24], where a method for a direct reduction is described that avoids leading inverse Gram determinants and the associated numerical instabilities. The remaining tensor integrals are recursively reduced to scalar integrals with the Passarino–Veltman algorithm [25] for non-exceptional phase-space points. In the exceptional phase-space regions the reduction of the 3- and 4-point tensor integrals is performed using the methods of Ref. [26] which allow for a numerically stable evaluation. The scalar integrals are calculated using the results of Refs. [27, 28]. For the numerical evaluation of the one-loop integrals we use a library by A. Denner implementing the methods of Refs. [24, 26].

The phase-space integration is performed with Monte Carlo techniques using the adaptive multi-dimensional integration program `Vegas` [29].

The correctness of our results was checked on the one hand by confirming their gauge invariance in the usual way, i.e. by replacing the external gluon polarization vector by the incoming momentum. On the other hand, the major part of the diagrams was independently calculated completely within `FeynArts/FormCalc/LoopTools` [21, 22, 23]. Of course, complete agreement was found among the two calculations.

Note that some of the diagrams, e.g. Fig. 5 (b), are singular as one or both of the outgoing partons become soft or collinear to the incoming parton(s). This cannot occur if we ask for the typical WBF signal which involves two hard jets, however. In fact, our minimal set of cuts imposed on the outgoing jets is

$$p_{Tj} > 20 \text{ GeV}, \quad |\eta_j| < 5, \quad R > 0.6, \quad j \in \{1, 2\}, \quad (1)$$

where p_{Tj} and η_j are the transverse momentum and the pseudo-rapidities of the final state jets, respectively. R is the separation of the jets in the η - ϕ plane,

$$R = \sqrt{(\Delta\eta)^2 + (\Delta\phi)^2}, \quad \Delta\eta = \eta_1 - \eta_2, \quad \Delta\phi = \phi_1 - \phi_2, \quad (2)$$

where ϕ_j is the azimuthal angle of the jet. Eq. (1) ensures that the events contain two well-separated hard jets at not too large rapidities.

The virtue of the WBF process is that a set of additional cuts on the outgoing jets allows for a significant improvement of the signal-to-background ratio, where “background” also includes Higgs production by other mechanisms than WBF, in particular by processes involving resonant gauge bosons. These so-called WBF cuts are given by Eq. (1) plus

$$\eta_1 \cdot \eta_2 < 0, \quad |\Delta\eta| > 4.2, \quad m_{jj} > 600 \text{ GeV}, \quad (3)$$

where m_{jj} is the invariant mass of the two-jet system. These cuts allow only for events in which the jets lie in opposite hemispheres of the detector, are separated by a significant rapidity gap, and have a large invariant mass.

IV. RESULTS

Since the SQL diagrams are a NNLO contribution to WBF we use the NNLO MRST2004 parton distributions [30] and a 2-loop running α_s . As the scale in the evaluation of both the PDFs and α_s we use $\mu = m_H$. The input parameters for the electro-weak sector are $\alpha = 1/137.036$, $m_W = 80.423 \text{ GeV}$, $m_Z = 91.1876 \text{ GeV}$ and $\sin^2 \theta_W = 0.222$.

For comparison, in Fig. 6 we show the total cross section for WBF at the LHC at LO and NLO QCD, both with the minimal set of cuts, Eq. (1), and with WBF cuts, Eq. (3). The curves were produced using the program `vbfnlo` [31]. One observes that the NLO corrections are of the order of 10%, and that the WBF cuts reduce the cross section by roughly a factor 2-3.

Fig. 7 shows the cross section due to the SQL contribution of Fig. 5. When minimal cuts are applied, the overall magnitude amounts to roughly 2% of the LO terms for $M_H = 100 \text{ GeV}$. However, the fall-off of the SQL contribution with increasing M_H is much steeper than for the conventional WBF process (note the logarithmic scale). Fig. 7 (b) shows the individual contributions from gg , qg , $\bar{q}g$, and $q\bar{q}$ initial states as they are obtained by crossing the external partons in Fig. 5. It is quite remarkable that the qg component dominates all the other channels by almost an order of magnitude.

WBF cuts suppress the SQL contribution by roughly a factor of 30, meaning that its effect on the WBF signal is completely negligible. The reason for this large suppression becomes clear once the relevant kinematical distributions are considered in more detail. Fig. 8 (a)

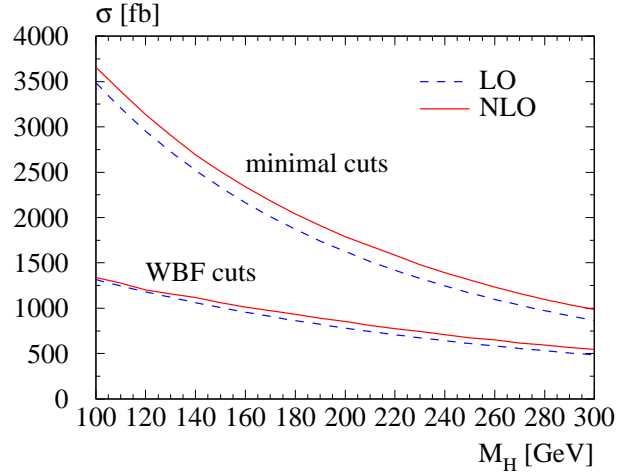


FIG. 6: (a) Total WBF cross section at the LHC at LO and NLO, both with the minimal set of cuts, Eq. (1), and with WBF cuts. Curves obtained using Ref. [31].

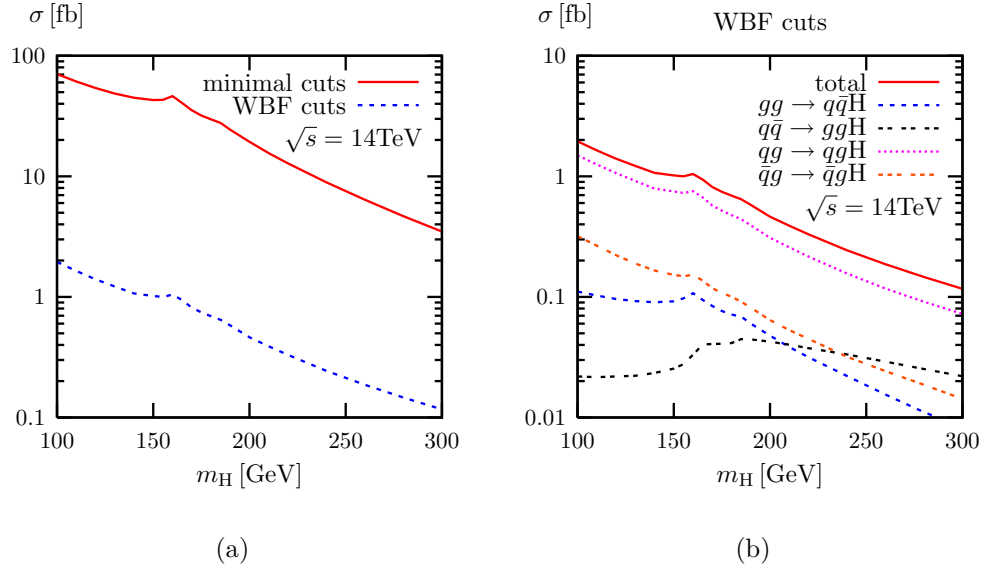


FIG. 7: (a) Total cross section at the LHC for the SQL contribution of Fig. 5 as a function of the Higgs mass m_H . Solid: with the minimal set of cuts, Eq. (1); dashed: with WBF cuts. (b) Individual contributions to the total cross section at the LHC when WBF cuts are applied.

and (b) show the distribution for the separation of the two jets when produced through SQL diagrams and the invariant mass of the two-jet system, respectively. The curves clearly show that the bulk of the events lies below the cuts of Eq. (3). In particular the cut on $|\Delta\eta|$ is extremely effective in removing this potentially dangerous component of the WBF process, thereby preserving its promising perspective for Higgs studies at the LHC.

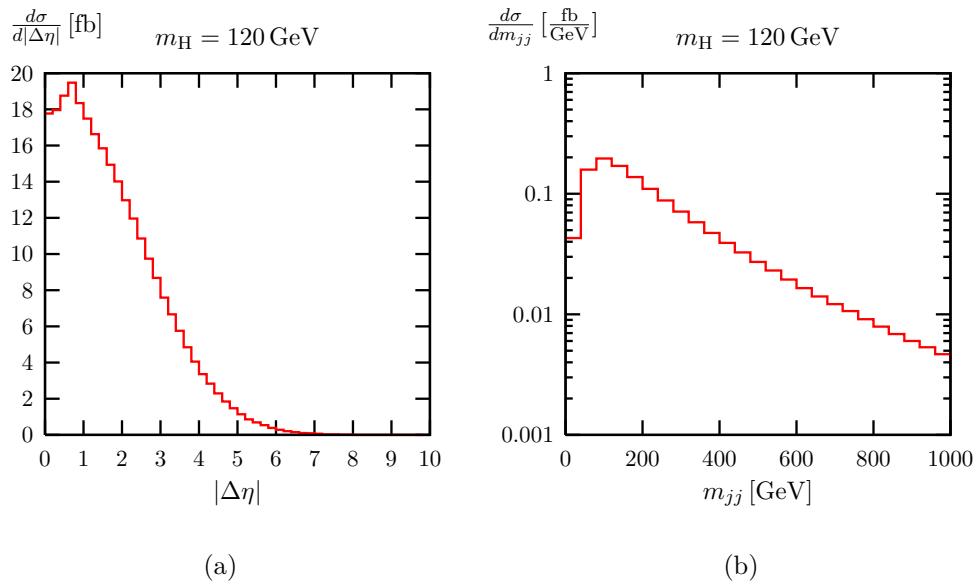


FIG. 8: Kinematical distributions of the final state jets for the SQL contribution using minimal cuts, Eq. (1).

V. CONCLUSIONS

WBF is a remarkable channel in the sense that the Higgs decay products are found in a region of the detector where hadronic activity is rather low. We have shown that for a potential source of such hadronic activity that occurs at NNLO, among them the purely gluon-initiated contribution, this statement remains true, because it is efficiently suppressed by the usual WBF cuts. In combination with recent results on interference effects with the gluon fusion process [17], this is a reassuring observation concerning the usefulness of the WBF process at the LHC.

Acknowledgments. We would like to thank A. Djouadi for initially pointing out this problem to us. We also thank him and T. Binoth for useful comments on the manuscript. R.H. acknowledges the hospitality of the *Galileo Galilei Institute* in Florence where part of this work was carried out. This work was financially supported by *Deutsche Forschungsgemeinschaft* under grants HA 2990/2-1 and HA 2990/3-1. The work of M.W. was supported in part by the National Science Foundation under grant NSF-PHY-0547564.

-
- [1] J.F. Gunion, H.E. Haber, G. Kane, S. Dawson, *The Higgs Hunter's Guide*, Addison-Wesley, 1990.
 - [2] A. Djouadi, hep-ph/0503172.
 - [3] A. Djouadi, hep-ph/0503173.
 - [4] LEP Electroweak Working Group, <http://lepewwg.web.cern.ch/LEPEWWG/>.

- [5] D.L. Rainwater and D. Zeppenfeld, *JHEP* **9712** (1997) 005, [hep-ph/9712271](#).
- [6] T. Han, G. Valencia, S. Willenbrock, *Phys. Rev. Lett.* **69** (1992) 3274, [hep-ph/9206246](#).
- [7] T. Figy, C. Oleari, D. Zeppenfeld, *Phys. Rev.* **D 68** (2003) 073005, [hep-ph/0306109](#).
- [8] E.L. Berger and J. Campbell, *Phys. Rev.* **D 70** (2004) 073011, [hep-ph/0403194](#).
- [9] M. Ciccolini, A. Denner, S. Dittmaier, *Phys. Rev. Lett.* **99** (2007) 161803, [arXiv:0707.0381 \[hep-ph\]](#); [arXiv:0710.4749 \[hep-ph\]](#).
- [10] M. Spira, *Fortschr. Phys.* **46** (1998) 203, [hep-ph/9705337](#).
- [11] A. Djouadi and M. Spira, *Phys. Rev.* **D 62** (2000) 014004, [hep-ph/9912476](#).
- [12] R.V. Harlander and W.B. Kilgore, *Phys. Rev. Lett.* **88** (2002) 201801, [hep-ph/0201206](#).
- [13] C. Anastasiou and K. Melnikov, *Nucl. Phys.* **B 646** (2002) 220, [hep-ph/0207004](#).
- [14] V. Ravindran, J. Smith, W.L. van Neerven, *Nucl. Phys.* **B 665** (2003) 325, [hep-ph/0302135](#).
- [15] V. Del Duca, W. Kilgore, C. Oleari, C. Schmidt, D. Zeppenfeld, *Phys. Rev. Lett.* **87** (2001) 122001; *Nucl. Phys.* **B 616** (2001) 367, [hep-ph/0105129](#); [hep-ph/0108030](#).
- [16] J.M. Campbell, R.K. Ellis, G. Zanderighi, *JHEP* **0610** (2006) 028, [hep-ph/0608194](#).
- [17] J.R. Andersen, T. Binoth, G. Heinrich, J.M. Smillie, [arXiv:0709.3513 \[hep-ph\]](#).
- [18] J.R. Andersen and J.M. Smillie, *Phys. Rev.* **D 75** (2007) 037301, [hep-ph/0611281](#).
- [19] E.B. Zijlstra and W.L. van Neerven, *Nucl. Phys.* **B 383** (1992) 525.
- [20] O. Brein, A. Djouadi, R. Harlander, *Phys. Lett.* **B 579** (2004) 149, [hep-ph/0307206](#).
- [21] J. Küblbeck, M. Böhm and A. Denner, *Comp. Phys. Commun.* **60** (1990) 165.
- [22] T. Hahn, *Comp. Phys. Commun.* **140** (2001) 418, [hep-ph/0012260](#).
- [23] T. Hahn and M. Perez-Victoria, *Comp. Phys. Commun.* **118** (1999) 153, [hep-ph/9807565](#).
- [24] A. Denner and S. Dittmaier, *Nucl. Phys.* **B 658** (2003) 175, [hep-ph/0212259](#).
- [25] G. Passarino and M.J.G. Veltman, *Nucl. Phys.* **B 160** (1979) 151.
- [26] A. Denner and S. Dittmaier, *Nucl. Phys.* **B 734** (2006) 62, [hep-ph/0509141](#).
- [27] G. 't Hooft and M. J. G. Veltman, *Nucl. Phys.* **B 153** (1979) 365.
- [28] A. Denner, U. Nierste and R. Scharf, *Nucl. Phys.* **B 367** (1991) 637.
- [29] G. P. Lepage, *J. Comp. Phys.* **27** (1978) 192.
- [30] A. D. Martin, R. G. Roberts, W. J. Stirling and R. S. Thorne, *Phys. Lett.* **B 604** (2004) 61, [hep-ph/0410230](#).
- [31] M. Bähr *et al.*, *VBFNLO — NLO parton level Monte Carlo for Vector Boson Fusion*, <http://www-itp.particle.uni-karlsruhe.de/~vbfnlweb/>